Polymer 50 (2009) 2328–2333

Contents lists available at ScienceDirect

Polymer

journal homepage: www.elsevier.com/locate/polymer

Miscibility and crystallization of biodegradable poly(butylene succinate-*co*-butylene adipate)/poly(vinyl phenol) blends

Fang Yang, Zhaobin Qiu*, Wantai Yang

State Key Laboratory of Chemical Resource Engineering, Beijing University of Chemical Technology, Beijing 100029, China

ARTICLE INFO

Article history:
Received 21 August 2008
Received in revised form
23 October 2008
Accepted 8 March 2009
Available online 26 March 2009

Keywords:
Biodegradable polymer blends
Miscibility
Crystallization

ABSTRACT

Miscibility, crystallization kinetics, crystal structure, and microstructure of biodegradable poly(butylene succinate-*co*-butylene adipate) (PBSA)/poly(vinyl phenol) (PVPh) blends were studied by differential scanning calorimetry, optical microscopy, wide angle X-ray diffraction, and small angle X-ray scattering in detail in this work. PBSA and PVPh are miscible as evidenced by the single composition dependent glass transition temperature and the negative polymer–polymer interaction parameter. Isothermal crystallization kinetics of PBSA/PVPh blends was investigated and analyzed by the Avrami equation. The overall crystallization rates of PBSA decrease with increasing crystallization temperature and the PVPh content in the PBSA/PVPh blends; however, the crystallization mechanism of PBSA does not change in the blends. Furthermore, blending with PVPh does not modify the crystal structure of PBSA. The microstructural parameters, including the long period, thickness of crystalline phase and thickness of amorphous phase, all become larger with increasing the PVPh content, indicating that PVPh mainly resides in the interlamellar region of PBSA spherulites in the blends.

1. Introduction

In recent years, conventional plastics have been widely used which caused severe environmental problems. Therefore, biodegradable polymers have received more and more attention. Biodegradable polymers can be classified into two types in terms of the preparation methods. One is biosynthetic polymers, such as bacterial polyhydroxyalkanoates (PHAs). The other is chemosynthetic polymers, such as the linear aliphatic polyesters. PBSA, a copolymer of poly(butylene succinate) (PBSU), is one of the biodegradable semicrystalline aliphatic polyesters. PBSA can be synthesized by polycondensation of 1,4-butanediol with succinic and adipic acids. The biodegradability, crystal structure, crystallization kinetics and melting behavior of PBSA have been reported in the literature [1–6]. Compared with PBSU, PBSA is more susceptible to biodegradation because of its lower crystallinity and more flexible polymer chains that can be easily biodegraded by enzymes.

Polymer blending is a simple and economic way to modify the physical properties and extend the practical application fields of biodegradable polymers. On the one hand, PBSA is miscible with poly(ethylene oxide) (PEO) and poly(vinylidene fluoride) (PVDF) [7–9]. The spherulitic growth of PEO was found to continue in the spherulites of PBSA in the simultaneous spherulitic growth process of the two components in the PBSA/PEO blends, resulting in the formation of interpenetrating spherulites [7]. In the PVDF/PBSA blends, the crystallization behavior of PBSA was affected by the presence of pre-existing crystals of PVDF. Three different types of crystalline morphologies for PBSA were found in the PVDF/PBSA blends [8,9]. On the other hand, PBSA is immiscible with poly(hydroxybutyrate) (PHB) and poly(L-lactic acid) (PLLA) [10,11]. In the PHB/PBSA blends, the crystal structure and crystallinity were almost the same as pure polymers [10]. In the PLLA/PBSA blends, the crystallization mechanism of PBSA did not change while the crystallization rate of PBSA decreased with increasing the PLLA content [11].

PVPh, an amorphous polymer with high glass transition temperature, is a proton donor which offers excellent potential for hydrogen bonding interactions with proton-acceptor polymers. PVPh is miscible with various polymers such as PEO [12–14], PHB [15,16], poly(hydroxyvalerate) (PHV) [17], PLLA [18], poly (ε-caprolactone) (PCL) [19], PBSU [20,21], poly(2-vinyl pyridine)-block-poly(ethylene oxide) (PVP-*b*-PEO) [22], and poly(ethylene succinate) (PES) [23]. The miscibility of polymer blends containing PVPh usually arises from the hydrogen bonding interaction between the hydroxyl group of PVPh and other groups of the partners, such as the carbonyl group. To the best of our knowledge, PBSA/PVPh blends have not been reported so far in the literature. In this work, miscibility, isothermal melt crystallization kinetics, crystal structure, and microstructure of PBSA/PVPh blends were studied by various techniques in detail.

* Corresponding author. Tel./fax: +86 10 64413161.
E-mail address: qiuzb@mail.buct.edu.cn (Z. Qiu).

0032-3861/$ – see front matter © 2009 Elsevier Ltd. All rights reserved.
doi:10.1016/j.polymer.2009.03.029

2. Experimental section

PBSA ($M_w = 14{,}400$) and PVPh ($M_w = 20{,}000$) were purchased from Aldrich Chemical Company and used as received. The Chemical structures of PBSA and PVPh are shown in Scheme 1. PBSA/PVPh blends were prepared with mutual solvent tetrahydrofuran. The solution of both polymers was cast on a petri dish at room temperature and was allowed to evaporate in a controlled air stream for 1 day. The resulting films were further dried in vacuum at 50 °C for 3 days. In this way, PBSA/PVPh blends were prepared with various compositions ranging from 90/10 to 20/80 in weight ratio, the first number referring to PBSA. The glass transition temperature (T_g) and the melting point (T_m) of the melt-quenched PBSA/PVPh blends were measured by a TA instruments differential scanning calorimetry (DSC) Q100 with a Universal Analysis 2000 at 20 °C/min. The samples were first annealed at 130 °C for 4 min to erase any thermal history and then quickly quenched into liquid nitrogen.

Isothermal crystallization kinetics of PBSA/PVPh blends was also investigated by DSC. We only studied neat PBSA and the blends with the weight fraction of PVPh less than 30% because PBSA did not crystallize or crystallized very slowly when the PVPh content was above 40 wt%. The samples were annealed at 130 °C for 4 min, cooled to the crystallization temperature (T_c) at a rate of 60 °C/min, and then maintained at T_c until the crystallization completed. The samples were scanned to 130 °C again at 20 °C/min to investigate the melting behavior of PBSA in the PBSA/PVPh blends.

Spherulitic morphology of PBSA/PVPh blends was observed under crossed polars with a polarizing microscope (POM) (Olympus BX51) equipped with a temperature controller (Linkam THMS 600). The samples were first annealed at 130 °C for 4 min to erase any thermal history and then cooled to 65 °C at 40 °C/min.

Wide angle X-ray diffraction (WAXD) experiments were performed on a SAXSess (Anton Paar company) using monochromatized CuKα radiation in the diffraction range $2\theta = 10$–$35°$. Small angle X-ray scattering (SAXS) measurements were carried out at room temperature with a NanoStar X-ray diffractometer (Bruker AXS, Inc.) using CuKα radiation ($\lambda = 0.154$ nm) at 40 kV and 30 mA. For the SAXS measurements, corrections were made for instrumental background. The samples for WAXD and SAXS measurements were prepared as follows. The samples were first pressed into films with thickness of around 1 mm on a hot stage at 130 °C for 3 min, transferred into an oven preset at 65 °C as soon as possible and held for 3 days.

3. Results and discussion

3.1. Miscibility study based on the glass transition temperature analysis

Miscibility of PBSA/PVPh blends was studied first by measuring the glass transition temperatures of the melt-quenched samples with DSC. Neat PBSA has a T_g of ca. −43.4 °C and a T_m of ca. 96.4 °C. On the other hand, neat PVPh is an amorphous polymer with a high

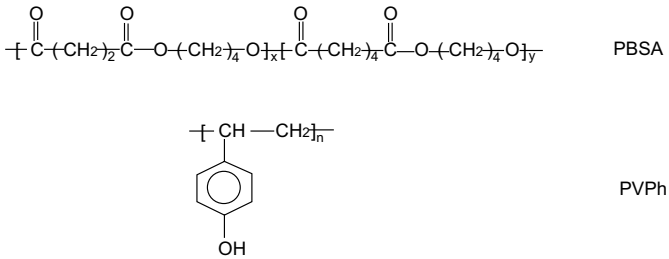

Scheme 1. The chemical structures of PBSA and PVPh.

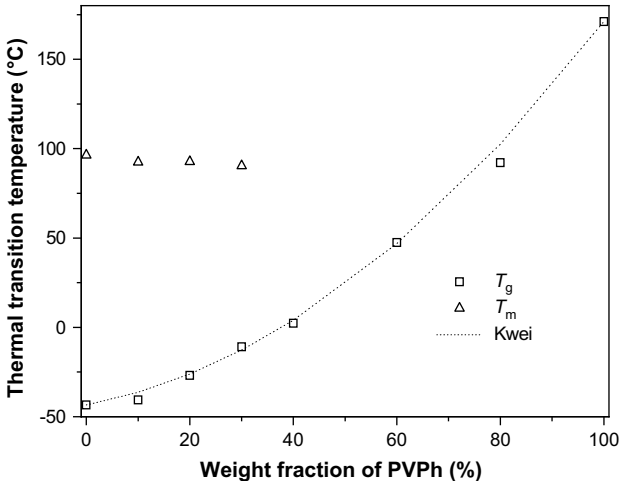

Fig. 1. Variation of T_g and T_m with the PVPh content in the PBSA/PVPh blends. (The dotted line is fitted by the Kwei equation.)

T_g of ca. 171.1 °C. Fig. 1 summarizes the variation of T_g and T_m with increasing the PVPh content. It can be seen from Fig. 1 that PBSA/PVPh blends show a single composition dependent T_g between those of the two neat components, indicating that PBSA and PVPh are miscible over the entire composition range. It is obvious that T_g of the PBSA/PVPh blends increases after blending with the high T_g component PVPh, resulting in the decrease of the mobility of PBSA in the blends. Therefore, the crystallization of PBSA is hindered by the presence of PVPh. As a result, T_m of PBSA shifts to low temperature range upon the addition of PVPh in the blends; however, the decrease of T_m is very slight. It should be noted that T_m of PBSA could not be detected with the PVPh content above 40 wt% in the blends.

Furthermore, the Kwei equation [24] is applied in this work to fit the variation of T_g as a function of composition as follows.

$$T_g = \frac{W_1 T_{g1} + kW_2 T_{g2}}{W_1 + kW_2} + qW_1 W_2 \quad (1)$$

where W_1 and W_2 are the weight fraction of two pure components, T_{g1} and T_{g2} are the respective T_g of the neat component, q is a parameter corresponding to the strength of hydrogen bonding in the blends, reflecting a balance between the breaking of the self-association and the forming of the inter-association hydrogen bonding, and k is a fitting constant. As showed in Fig. 1, the Kwei equation fits T_g of PBSA/PVPh blends very well. In this work, a negative q of −160 is obtained in the case of $k = 1$, which is greatly lower than that of −85 for PCL/PVPh blends [19], indicating that the interaction between PBSA and PVPh is weaker than that in the PCL/PVPh blends.

3.2. The depression of the equilibrium melting point of PBSA in the PBSA/PVPh blends

The depression of the melting point of crystalline polymer blended with an amorphous polymer provides important information of its miscibility. An immiscible blends or partially miscible blends do not show the depression of melting point significantly. However, the melting point of a polymer is affected not only by the thermodynamic factors but also by the morphological factors such as crystalline lamellar thickness and the perfection of spherulites. Therefore, the equilibrium melting point (T_m^o) is introduced to separate the morphological effect from the thermodynamic effect in discussing the melting point depression as described by the

Flory–Huggins theory [25]. T_m^o can be derived from the Hoffmann–Weeks equation [26]:

$$T_m = \eta T_c + (1-\eta)T_m^o \quad (2)$$

where T_m is the apparent melting point, T_c is the crystallization temperature, and η may be regarded as a measure of the stability.

The melting behavior of PBSA/PVPh blends was studied with DSC. As an example, Fig. 2a shows the melting behavior of a 90/10 blend crystallized isothermally at various T_cs. Two endothermic melting peaks are observed. The lower endothermic peak (T_{m1}) shifts to higher temperature range with increasing T_c, while the higher endothermic peak (T_{m2}) is almost unchanged. Moreover, the magnitude of the area of T_{m1} increases and that of T_{m2} decreases with the increase of T_c. This is also observed in the 80/20 and 70/30 blends. Such melting behavior can be explained by the melt-recrystallization model [7,27–29]. T_{m1} is the melting of crystals formed during the isothermal crystallization process which are present prior to the heating scan, and dependent greatly on T_c; T_{m2} is the melting of the crystals formed through the recrystallization during the heating process.

Therefore, T_{m1} is used for the analysis of the Hoffman–Weeks equation. Fig. 2b shows the Hoffman–Weeks plots for neat PBSA and the blends. From Fig. 2b, the values of T_m^os are determined to be around 120.0, 113.2, 102.6, and 100.6 °C for neat PBSA, 90/10, 80/20, and 70/30 blends, respectively. It is clear that T_m^o of PBSA decreases with increasing the PVPh content. The depression of T_m^o indicates again that PBSA and PVPh are miscible polymer blends. T_m^os obtained on this study is further analyzed by the Nishi–Wang equation [30] based on the Flory–Huggins theory [25]:

$$\frac{1}{T_m^o(b)} - \frac{1}{T_m^o(p)} = -\frac{RV_2}{\Delta H^o V_1}\left[\frac{\ln\phi_1}{m_2} + \left(\frac{1}{m_2} - \frac{1}{m_1}\right)\phi_1 + \chi_{12}\phi_1^2\right] \quad (3)$$

where $T_m^o(p)$ and $T_m^o(b)$ are the equilibrium melting points of the pure crystallizable polymer and of the blend, respectively. ΔH^o is the fusion heat of the perfectly crystallizable polymer per mole of the repeat unit, V is the molar volume of the repeating units of the polymers, m and ϕ are degree of polymerization and the volume fraction of the component in the blends, respectively. Subscripts 1 and 2 refer to the amorphous and crystalline polymer, respectively. R is the universal gas constant, and χ_{12} is the polymer–polymer interaction parameter. When both m_1 and m_2 are large, for high molecular weight polymers, these related terms in Eq. (3) can be neglected. The interaction parameter χ_{12} can thus be written as

$$\frac{\Delta H^o V_1}{RV_2}\left(\frac{1}{T_m^o(b)} - \frac{1}{T_m^o(p)}\right) = \beta = \chi_{12}\phi_1^2 \quad (4)$$

In order to calculate the left-hand side term of Eq. (4), the following parameters are used: $V_1 = 100\ \mathrm{cm^3/mol}$ [31], $V_2 = 135.1\ \mathrm{cm^3/mol}$, and $\Delta H^o = 20,304\ \mathrm{J/mol}$ [32]. The weight fraction of amorphous polymer is transformed to volume fraction. The plot of the left-hand of Eq. (4) versus ϕ_1^2 is shown in Fig. 3, from which the value of χ_{12} is obtained as −0.82. The value of χ_{12} is negative, indicating that PBSA and PVPh are thermodynamically miscible. In the PBSA/PVPh blends, χ_{12} is found to be −0.82, which is higher than −1.4 in the PHB/PVPh blends and −1.5 in the PEO/PVPh blends [14,16]. It indicates that the interaction between PBSA and PVPh is much weaker than those in the PHB/PVPh blends and the PEO/PVPh blends.

3.3. Isothermal crystallization of PBSA/PVPh blends

Isothermal crystallization kinetics of PBSA/PVPh blends was investigated by DSC. Fig. 4a shows the variation of relative crystallinity with crystallization time for a PBSA/PVPh 90/10 blend. It can be seen that the crystallization isotherms display the characteristic sigmoidal shape. Moreover, the crystallization time

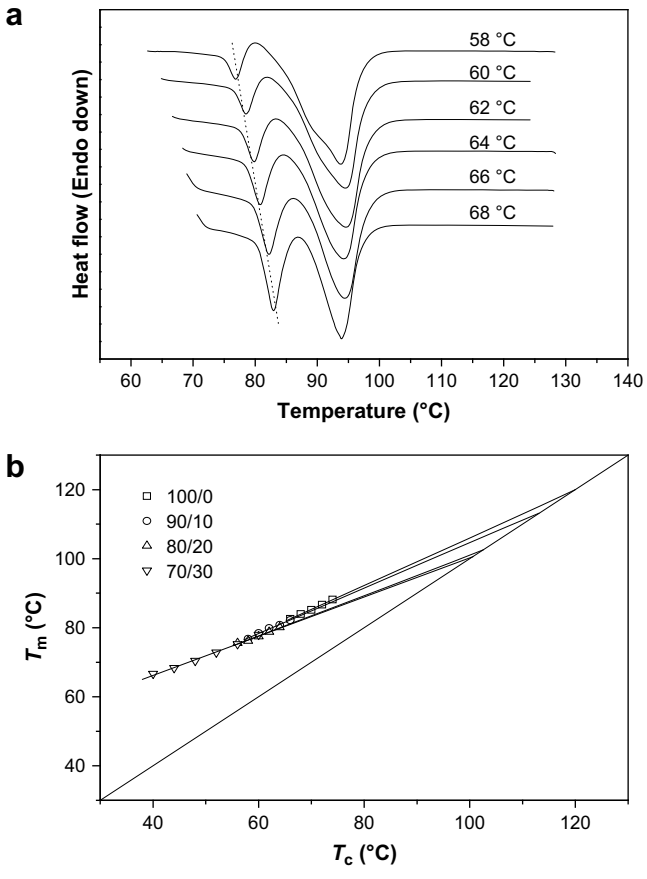

Fig. 2. (a) Melting behavior of a 90/10 blend isothermally crystallized at various T_cs from the melt; (b) Hoffman–Weeks plots of neat and blended PBSA for the estimation of the equilibrium melting points.

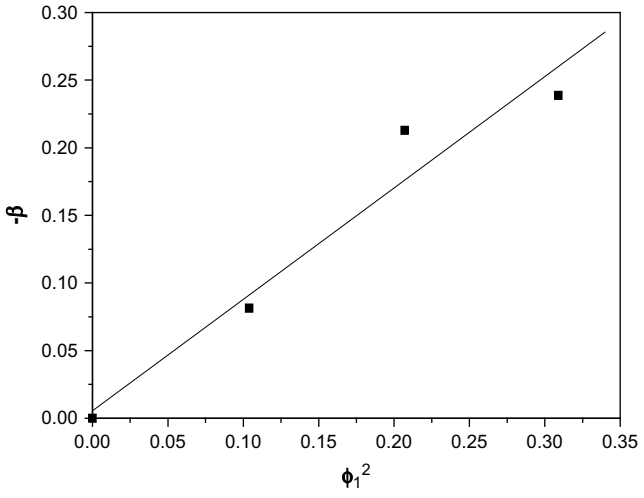

Fig. 3. Nishi–Wang plot for the calculation of the polymer–polymer interaction parameter of PBSA/PVPh blends.

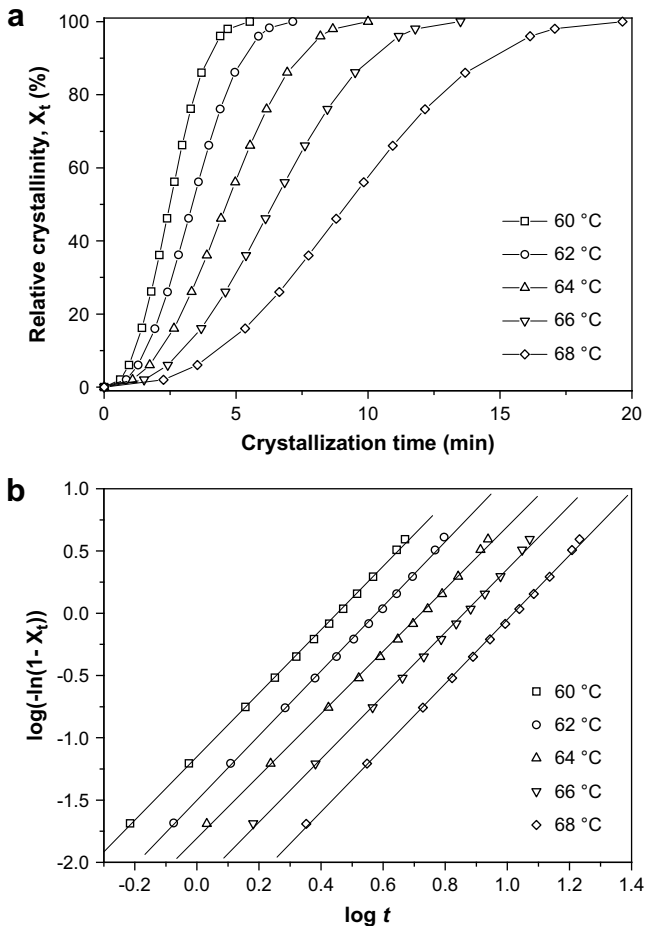

Fig. 4. (a) Development of relative crystallinity X_t versus crystallization time; (b) Avrami plots of a PBSA/PVPh 90/10 blend.

prolongs with the increase of crystallization temperature for both neat and blended PBSA.

The Avrami equation is usually employed to analyze the isothermal crystallization kinetics of crystalline polymers, which describes the development of relative degree of crystallinity with crystallization time t as

$$1 - X_t = \exp(-kt^n) \quad (5)$$

where X_t is the relative crystallinity at time t, k is the crystallization rate constant depending on nucleation and growth rate, and n is the Avrami exponent depending on the nature of nucleation and growth geometry of the crystals [33–35].

Fig. 4b shows the Avrami plots for a PBSA/PVPh 90/10 blend. It can be seen that a series of straight lines are obtained, which indicates that the Avrami method can describe the development of the relative degree of crystallinity as a function of crystallization time very well. Accordingly, the Avrami parameters n and k can be obtained from the slopes and intercepts, respectively. The values of n and k for neat and blended PBSA are summarized in Table 1. The values of n of neat PBSA and PBSA blends are between 2 and 3, suggesting that the crystallization of PBSA may correspond to three-dimensional truncated spherulitic growth with athermal nucleation [36]. Furthermore, blending with PVPh does not change the crystallization mechanism of PBSA in the blends apparently.

The half-time of crystallization ($t_{0.5}$), defined as the time required to half completion of the final crystallinity, can be obtained by Eq. (6). The overall crystallization rate can be simply represented by $1/t_{0.5}$.

$$t_{0.5} = \left(\frac{\ln 2}{k}\right)^{1/n} \quad (6)$$

Table 1
Isothermal crystallization kinetics parameters of neat and blended PBSA.

	T_c (°C)	n	k (min^{-n})	$t_{0.5}$ (min)
100/0	62	2.7	3.3×10^{-1}	1.3
	64	2.3	1.6×10^{-1}	1.9
	66	2.5	3.1×10^{-2}	3.4
	68	2.7	6.0×10^{-3}	5.7
	70	2.6	4.0×10^{-3}	7.2
90/10	60	2.6	7.0×10^{-1}	2.4
	62	2.6	2.8×10^{-2}	3.5
	64	2.5	1.3×10^{-2}	4.9
	66	2.5	6.5×10^{-3}	6.3
	68	2.6	2.4×10^{-3}	9.1
80/20	60	2.1	1.9×10^{-2}	5.4
	62	2.5	4.2×10^{-3}	8.0
	64	2.5	2.3×10^{-3}	10.1
	66	2.4	1.9×10^{-3}	11.0
	68	2.3	1.2×10^{-3}	15.1
70/30	44	2.2	2.7×10^{-1}	1.5
	48	2.1	7.9×10^{-2}	2.8
	52	2.4	3.9×10^{-2}	3.3
	56	2.0	2.0×10^{-2}	5.8
	60	2.3	1.7×10^{-3}	14.0

On the basis of the values of n and k, the values of $t_{0.5}$ and $1/t_{0.5}$ were calculated. Table 1 summarizes the values of $t_{0.5}$ for both neat and blended PBSA. It is obvious that the values of $t_{0.5}$ increase with the increase of T_c for both neat PBSA and its blends with PVPh at different content. Moreover, it is also found that the values of $t_{0.5}$ are smaller in the neat PBSA than those in the blends at a given T_c, indicating that the crystallization rate of PBSA becomes slower after blending with PVPh.

In order to show the effects of blend composition and crystallization temperature on the crystallization rate of PBSA clearly, Fig. 5 summarizes the temperature dependence of $1/t_{0.5}$ for neat PBSA and its blends with different contents of PVPh. From Fig. 5, the overall crystallization rates of PBSA decrease with increasing T_c for both neat and blended PBSA, resulting from the difficulty in nucleation at high T_c. On the other hand, the overall crystallization

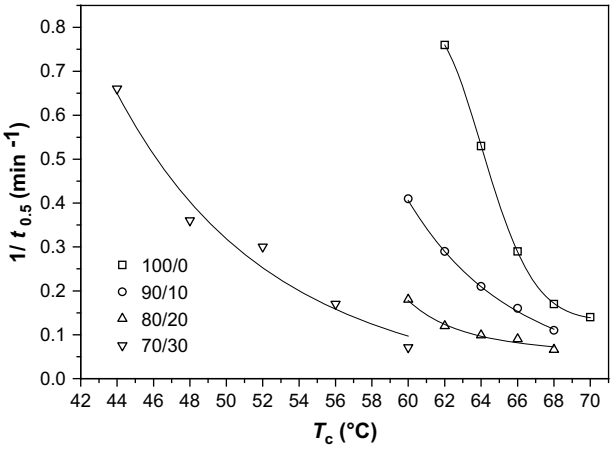

Fig. 5. Crystallization temperature dependence of $1/t_{0.5}$ for neat and blended PBSA.

rates decrease with increasing the PVPh content at a given T_c, indicating that blending with amorphous PVPh retards the crystallization of PBSA in the blends. The reduction of the crystallization rate of PBSA in the blends may be attributed to the following factors. First, the addition of high T_g component PVPh increases T_gs of PBSA/PVPh blends, resulting in the decrease of the mobility of PBSA compared with that of neat PBSA. Second, the equilibrium melting point temperatures of blended PBSA were lower than that of neat PBSA, which must drop the thermodynamic driving force required for the crystallization of PBSA. Third, the addition of PVPh may play a role of a diluent to PBSA in the miscible blends, resulting in the dilution of PBSA chains at the spherulites growth front [21,23,38].

Fig. 6 shows POM images of neat and blended PBSA crystallized at 65 °C. The spherulites of neat PBSA are compact. In the case of the PBSA/PVPh blends, PBSA spherulites become coarser compared with those of neat PBSA. For an 80/20 blend, the bundles of lamellae are fewer but thicker than those for neat PBSA, and assume a feather-like pattern. The fact that PBSA spherulites are space-filling indicates that PVPh is rejected in the crystallization process and may reside primarily in the fibrillar and lamellar domains of PBSA spherulites.

3.4. WAXD and SAXS studies of neat and blended PBSA

The crystal structure and microstructure of PBSA before and after blending with PVPh were investigated with WAXD and SAXS in the present work. Fig. 7 shows the WAXD patterns of neat and blended PBSA crystallized at 65 °C for 3 days. It can be seen from Fig. 7 that both neat and blended PBSA exhibit almost the same diffraction peaks at the same location. However, the intensity of the diffraction peaks decreases with increasing the PVPh content. It indicates that blending with amorphous PVPh does not modify the crystal structure of PBSA, but decreases the crystallinity of PBSA in the blends.

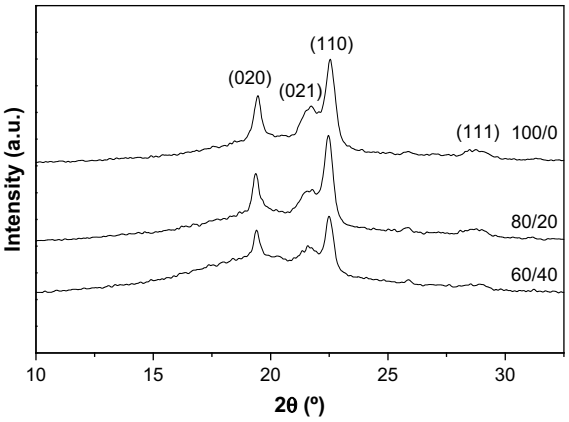

Fig. 7. WAXD patterns of neat and blended PBSA crystallized at 65 °C for 3 days.

The microstructure of the PBSA/PVPh blends was studied by SAXS. The morphological parameters in the lamellar level, such as long period (*LP*), crystal layer thickness (L_c), and amorphous layer thickness (L_a) are determined by one-dimensional correlation function [37],

$$\gamma(z) = \frac{1}{\gamma(0)} \int_0^\infty I(q) q^2 \cos(qz) \mathrm{d}q \tag{7}$$

where z is the correlation distance, $\gamma(0)$ is the scattering invariant, q is the scattering vector, which was calculated from $q = 4\pi \sin\theta/\lambda$ ($\lambda = 0.154$ nm), 2θ is the scattering angle, and I is the scattering intensity distributions.

The curves of normalized one-dimensional correlation function $\gamma(z)$ are shown in Fig. 8 for neat and blended PBSA. From Fig. 8, the values of *LP*, L_c and L_a are obtained. Fig. 9 summarizes the variation of *LP*, L_c and L_a for both neat PBSA and its blends with different PVPh contents.

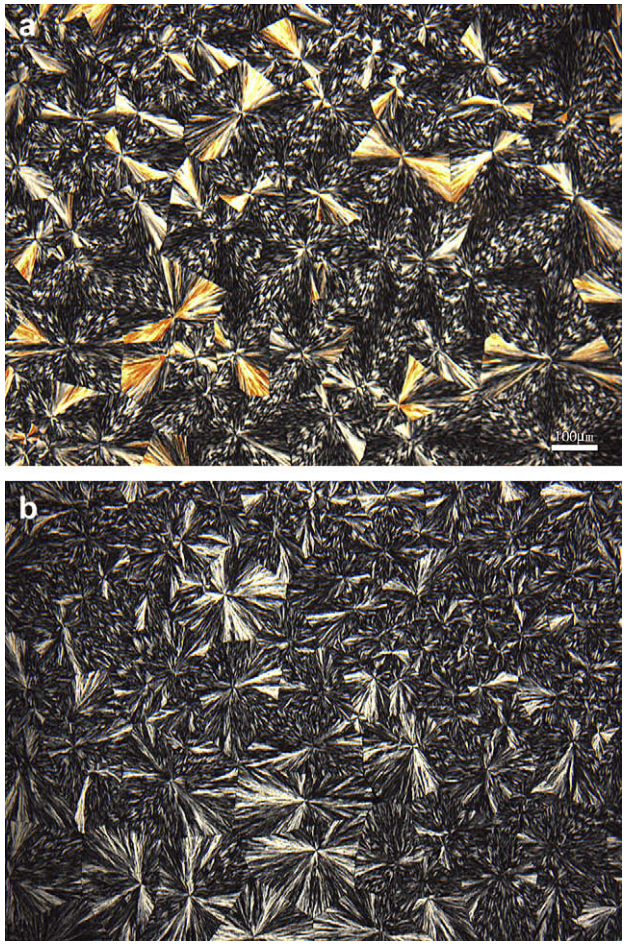

Fig. 6. Optical micrographs (same magnification with bar = 100 μm) of the spherulitics morphology of neat PBSA and an 80/20 blend crystallized at 65 °C (a) 100/0; (b) 80/20.

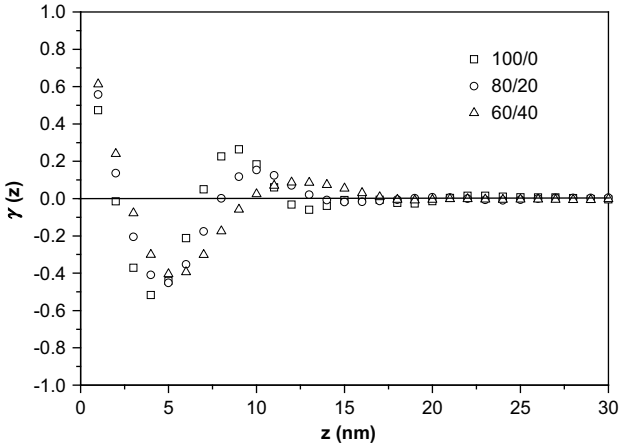

Fig. 8. One-dimensional correlation function curves of $\gamma(z)$ for neat and blended PBSA crystallized at 65 °C for 3 days.

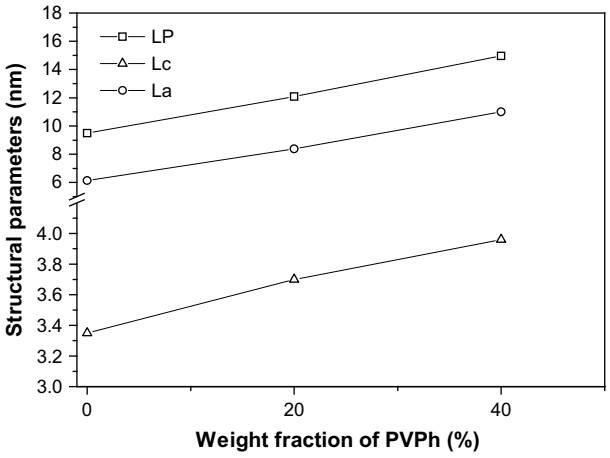

Fig. 9. Variation of microstructural parameters with PVPh content for the PBSA/PVPh blends crystallized at 65 °C for 3 days: (□) long period; (○) crystal layer thickness; and (△) amorphous layer thickness.

As shown in Fig. 9, the values of *LP*, L_c and L_a are 9.49, 3.35 and 6.14 nm, respectively, for neat PBSA. For an 80/20 blend, they increase to be 12.09, 3.70 and 8.39 nm, respectively. With further increasing the PVPh content, they become 14.96, 3.96 and 11.0 nm, respectively, in the case of a 60/40 blend. It is obvious that all the values of *LP*, L_c and L_a of PBSA increase with increasing the PVPh content in the PBSA/PVPh blends. It should be noted that the increase in L_c is very small. For example, the increase is only around 0.6 nm with increasing the PVPh content up to 40 wt% in the blends. However, the increase in L_a is large. For example, the increase in L_a is around 2.2 nm after blending 20 wt% PVPh as compared to that of neat PBSA. The increase in L_a is around 4.8 nm with further increasing the PVPh content up to 40 wt% in the blend as compared to that of neat PBSA. Such significant increase in L_a indicates that amorphous PVPh may mainly reside in the interlamellar region of PBSA spherulites. Accordingly, the *LP* values increase from 9.49 for neat PBSA to 12.09 and 14.96 nm for the 80/20 and 60/40 blends, respectively. The increase in *LP* mainly arises from the increase in L_a although there is also a small increase in L_c in the PBSA/PVPh blends. Similar results were also found in PCL/phenolic blends [38].

4. Conclusions

Miscibility, isothermal crystallization kinetics, crystal structure, and microstructure of biodegradable PBSA/PVPh blends were investigated with DSC, POM, WAXD, and SAXS in detail in this work. The following conclusions are obtained:

(1) PBSA and PVPh are miscible crystalline/amorphous polymer blends. Miscibility of PBSA/PVPh blends is evidenced by the single composition dependent glass transition temperature over the entire blend compositions. The negative polymer–polymer interaction parameter, obtained from the melting depression of PBSA using the Nishi–Wang equation, further indicates that PBSA/PVPh blends are thermodynamically miscible.

(2) Isothermal crystallization kinetics study of neat and blended PBSA indicates that the crystallization mechanism of PBSA does not change, but the crystallization rate decreases with increasing the PVPh content in the blends.

(3) The crystal structure of PBSA is not modified in the PBSA/PVPh blends. However, the values of *LP*, L_c, and L_a become larger with increasing the PVPh content, indicating that PVPh mainly resides in the interlamellar region of PBSA spherulites.

Acknowledgements

Part of this work is financially supported by the National Natural Science Foundation, China (Grant Nos. 20504004 and 20774013), Program for New Century Excellent Talents in University (NCETf-06-0101), and Program for Changjiang Scholars and Innovative Research Team in University (IRT0706).

References

[1] Tserki V, Matzinos P, Pavlidou E, Vachliotis D, Panayiotou C. Polym Degrad Stab 2006;91:367.
[2] Tserki V, Matzinos P, Pavlidou E, Vachliotis D, Panayiotou C. Polym Degrad Stab 2006;91:377.
[3] Chatani Y, Hasegawa R, Tadokoro H. Polym Prepr Jpn 1971;20:420.
[4] Ihn K, Yoo E, Im S. Macromolecules 1995;28:2460.
[5] Ichikawa Y, Kondo H, Igarashi Y, Noguchi K, Okuyama K, Washiyama J. Polymer 2000;41:4719.
[6] Ren M, Song J, Song C, Zhang H, Sun X, Chen Q, et al. J Polym Sci Part B Polym Phys 2005;43:3231.
[7] Ikehara T, Kimura H, Qiu Z. Macromolecules 2005;38:5104.
[8] Qiu Z, Yan C, Lu J, Yang W. Macromolecules 2007;40:5047.
[9] Qiu Z, Yan C, Lu J, Yang W, Ikehara T, Nishi T. J Phys Chem B 2007;111:2783.
[10] He Y, Masuda T, Cao A, Yoshie N, Doi Y, Inoue Y. Polym J 1999;31:184.
[11] Wang Y, Mano J. J Appl Polym Sci 2007;105:3204.
[12] Pedrosa P, Pomposo J, Calahorra E, Cortazar M. Polymer 1995;36:3889.
[13] Huang Y, Kuo J, Woo E. Polym Int 2001;51:55.
[14] Qin C, Pires A, Belfiore L. Polym Commun 1990;31:177.
[15] Iriondo P, Iruin J, Fernandez-Berridi M. Polymer 1995;36:3235.
[16] Xing P, Dong L, An Y, Feng Z, Avlla M, Martuscelli E. Macromolecules 1997;30:2726.
[17] Zhang L, Goh S, Lee S. J Appl Polym Sci 1999;74:383.
[18] Zhang L, Goh S, Lee S. Polymer 1998;39:4841.
[19] Kuo S, Huang C, Chang F. J Polym Sci Part B Polym Phys 2001;39:1348.
[20] Qiu Z, Komura M, Ikehara T, Nishi T. Polymer 2003;44:8111.
[21] Qiu Z, Yang W. Polymer 2006;47:6429.
[22] Lee L, Woo E, Hou S, Förster S. Polymer 2006;47:8350.
[23] Qiu Z, Fujinami S, Komura M, Nakajima K, Ikehara T, Nishi T. Polymer 2004;45:4515.
[24] Kwei T. J Polym Sci Polym Lett Ed 1984;22:307.
[25] Flory P. Principles of polymer chemistry. Ithaca, New York: Cornell University Press; 1953.
[26] Hoffman J, Weeks J. J Chem Phys 1965;42:4301.
[27] Wang X, Zhou J, Li L. European Polym J 2007;43:3163.
[28] Yoo E, Im S. J Polym Sci Part B Polym Phys 1999;37:1357.
[29] Yasuniwa M, Tsubakihara S, Satou T, Iura K. J Polym Sci Part B Polym Phys 2005;43:2039.
[30] Nishi T, Wang TT. Macromolecules 1975;8:909.
[31] Coleman M, Lichkus A, Painter P. Macromolecules 1989;22:586.
[32] Marija S, Jasna D. Polymer Degradation and Stability 2001;74:263.
[33] Avrami M. J Chem Phys 1939;7:1130.
[34] Avrami M. J Chem Phys 1940;8:212.
[35] Avrami M. J Chem Phys 1941;9:177.
[36] Wunderlich B. Macromolecular physics, crystal nucleation, growth, annealing, vol. II. New York: Academic Press; 1976.
[37] Strobl G, Schneider M. J Polym Sci Polym Phys Ed 1980;18:1343.
[38] Kuo S, Chan S, Chang F. J Polym Sci Part B Polym Phys 2004;42:117.